Direct assessment of quantum nuclear effects on hydrogen bond strength by constrained-centroid *ab initio* path integral molecular dynamics

Brent Walker and Angelos Michaelides[a)]
Department of Chemistry and London Centre for Nanotechnology, University College London, London WC1E 6BT, United Kingdom

(Received 20 August 2010; accepted 4 October 2010; published online 2 November 2010)

The impact of quantum nuclear effects on hydrogen (H-) bond strength has been inferred in earlier work from bond lengths obtained from path integral molecular dynamics (PIMD) simulations. To obtain a direct quantitative assessment of such effects, we use constrained-centroid PIMD simulations to calculate the free energy changes upon breaking the H-bonds in dimers of HF and water. Comparing *ab initio* simulations performed using PIMD and classical nucleus molecular dynamics (MD), we find smaller dissociation free energies with the PIMD method. Specifically, at 50 K, the H-bond in $(HF)_2$ is about 30% weaker when quantum nuclear effects are included, while that in $(H_2O)_2$ is about 15% weaker. In a complementary set of simulations, we compare unconstrained PIMD and classical nucleus MD simulations to assess the influence of quantum nuclei on the structures of these systems. We find increased heavy atom distances, indicating weakening of the H-bond consistent with that observed by direct calculation of the free energies of dissociation. © *2010 American Institute of Physics*. [doi:10.1063/1.3505038]

I. INTRODUCTION

It is not difficult to illustrate the importance of hydrogen (H-) bonds in nature—cases where H-bonds play a major role include the structures of liquid water and ice, and the binding of the strands of base pairs in DNA.[1] Correspondingly, H-bonding has remained a major research topic; an ongoing example is the discussion of H-bonding in the structure of liquid water.[2–13] Although it is often possible to avoid explicit consideration of the quantum mechanics of the nuclei in simulations,[14] when atoms having light nuclei are involved, quantifiable deviations from the picture of the nuclei as classical point particles can occur, especially at low temperatures. Examples include the structure of ice and proton transfer in liquid water, ice, and water at interfaces.[15] The covalent bond lengths in the water molecule itself are affected by the mass of hydrogen.[16] Undoubtedly, it is important to assess quantum nuclear effects in the case of H-bonds, where light nuclei are intrinsically involved. By considering pair correlation functions from path integral molecular dynamics (PIMD) simulations, it has been suggested that the H-bonds in liquid water are weakened by quantum nuclear effects.[13] This differs from the behavior seen in bulk liquid hydrogen fluoride (HF), where PIMD simulations indicated that the quantum mechanics of the nuclei strengthens H-bonding.[17] For dimers of both water and HF, assessments of quantum nuclear effects on the heavy atom distances indicated weakening of the H-bonds.[18,19] In the case of HF clusters, PIMD calculations suggested a crossover from weakening to strengthening of the H-bonding in clusters of more than four HF monomers due to quantum nuclear effects.[19]

In these earlier studies, the influence of quantum nuclear effects on H-bond strength was inferred indirectly from the structural data: bond lengths in the case of small clusters and pair correlation functions in the case of bulk systems. To directly assess quantum nuclear effects on H-bond strength, it is important to consider the free energy changes involved with breaking the H-bonds. There are several ways to calculate free energies. A computationally efficient method to determine free energy changes involved with a transition, such as the dissociation of an H-bond, is the potential of mean force (PMF).[20–23] This method is attractive in the context of quantum nuclei as it was shown to seamlessly translate to the PIMD context in the work of Gillan.[24] Here, we directly determine the influence of quantum nuclear effects on the strengths of H-bonds by comparing PMFs obtained with classical and quantum nuclei. As test cases, we consider HF and water dimers at low temperature (50 K). In the PIMD case, we employ a simple scheme to constrain the centroids (geometrical averages of the positions of the atoms over all the beads representing the system). To assess the influence of quantum nuclear effects on the equilibrium structures of these dimers, we also perform unconstrained PIMD and classical nucleus MD simulations for the same systems. For both MD and PIMD simulations, all interatomic interactions are determined using density functional theory (DFT). Although the computational cost of accurately including quantum nuclear effects in the calculation of dissociation free energies is still substantial, our work shows that, in general, it is now feasible to directly compute the strengths of H-bonds using *ab initio* PIMD.

This paper proceeds as follows. First, we describe our methodology, in particular, outlining the constrained-centroid PIMD method we use to calculate PMFs with quantum nuclei. We then move to the main part of the work, in which we consider small H-bonded systems, presenting PIMD and

a)Electronic mail: angelos.michaelides@ucl.ac.uk.

 © 2010 American Institute of Physics

Author complimentary copy. Redistribution subject to AIP license or copyright, see http://jcp.aip.org/jcp/copyright.jsp

classical nucleus MD mean forces for dimers of HF and water at 50 K, together with the resulting dissociation free energies. Such mean force curves for the dissociation of H-bonded dimers have not previously been obtained with *ab initio* PIMD. For the HF dimer, the mean constraint forces in the PIMD case are significantly smaller in magnitude than in the classical nucleus MD calculations, leading to a reduction of ~30% in the H-bond strength. We examine the effect of replacing the hydrogen atoms in $(HF)_2$ with deuterium (D) atoms, finding that the free energy of dissociation is reduced by ~10% in the PIMD simulations, a smaller reduction than that seen in the case of $(HF)_2$. For the water dimer, we again find a reduction (~15%) of the free energy of dissociation when quantum nuclear effects are included; when the H atoms are replaced by D atoms, the reduction in the free energy of dissociation due to quantum nuclear effects becomes ~10%. Next, we discuss the free energies of dissociation obtained with our PIMD and classical nucleus MD approaches in light of other estimates of the energies involved in dissociating these H-bonded dimers and summarize our findings. Overall, this work establishes a clear connection between increased heavy atom distances and weakening of H-bonds due to quantum nuclear effects.

II. METHODS

The PIMD formalism[14,25] is a computationally tractable way to describe the full quantum mechanics of a system, avoiding the approximation that the nuclei are point particles, which is often made in atomistic simulation work. A set of replicas or "beads" coupled by harmonic springs (with temperature- and mass-dependent spring constants) represents the system in a description resembling a ring polymer. An equilibrium sampling of the set of coupled beads provides the full partition function of the system, with the nuclei treated as quantum particles. For each atom, the geometrical average of its position over all the beads is termed its *centroid*. Energy barriers and rates for reactions and transitions, including proton transfers, have previously been studied using PIMD techniques,[26–29] often via centroid molecular dynamics,[30–35] an approximate scheme that works with the centroids as classical dynamical variables, subject to a mean potential energy surface. Another PIMD-based scheme that has recently been used to estimate reaction rates and real-time correlation functions is the ring-polymer molecular dynamics method.[35–39]

In the present work, the internal energy of each PIMD bead is calculated using DFT. We use ultrasoft pseudopotentials,[40] with plane wave basis sets,[41] periodic boundary conditions, and the supercell approach[42] in performing the DFT calculations for each bead. The Perdew–Burke–Ernzerhof (PBE) (Ref. 43) exchange-correlation functional is used in all cases. We use the CASTEP plane wave DFT code.[44] Extensive studies have benchmarked the reliability of modern electronic structure methods for studying H-bonds. In particular, the results of using DFT with various exchange-correlation functionals for calculating the structures and dissociation energies of many H-bonded complexes have been compared with quantum chemistry calculations and experimental results in several works.[45–51] The PBE functional works reasonably well for intermediate strength H-bonds in small clusters such as those under consideration here. This can be seen in Table I, where the equilibrium dissociation energies D_e (Ref. 52) and harmonic zero-point energy (ZPE) corrected dissociation energies D_0 (Ref. 53) for the HF and water dimers are compared to those obtained with coupled-cluster theory [CCSD(T)] in the literature. Table I shows that for both $(HF)_2$ and $(H_2O)_2$, the plane wave PBE values are within ~40 meV of the CCSD(T) results. Part of this error can be attributed to the particular pseudopotentials and plane wave basis sets employed. This setup is adequate for the present purpose of comparing systems with classical and quantum nuclei but does not yield dissociation energies with meV precision compared to accurate all electron results.[49]

TABLE I. Equilibrium dissociation energies D_e (upper part) (Ref. 52) and harmonic ZPE-corrected dissociation energies D_0 (lower part) for HF and water dimers calculated with various methods. The electronic structure method is indicated in each case.

	D_e (eV)	
	$(HF)_2$	$(H_2O)_2$
PBE[a]	0.238	0.232
PBE[b]	0.209	0.214
CCSD(T)[c]		0.218
CCSD(T)[d]	0.199	
	D_0 (eV)	
	$(HF)_2$	$(H_2O)_2$
PBE[a]	0.153	0.122
PBE[b]	0.131	0.122
CCSD(T)[e]		0.143
CCSD(T)[f]	0.133	

[a]Plane waves: E_{cut}=400 eV (this work).
[b]aug-cc-pV5Z (this work).
[c]cc-pVQZ (Ref. 54).
[d]aug-cc-pVxZ (Ref. 55).
[e]QQZ (Ref. 56).
[f]cc-pVQZ (Ref. 55).

To calculate free energy profiles for the dissociation of H-bonds, we appeal to the PMF.[20–23] PMFs have proved popular in considering free energy barriers, especially for reactions,[57] and have been used to study H-bonds with classical nuclei.[58,59] For a system of N particles having coordinates $\{\mathbf{r}_1,\ldots,\mathbf{r}_N\}$, the PMF, $w^{(n)}$, associated with holding a subset $1,\ldots,n$ of those particles fixed is defined as the average gradient of the system potential over all configurations of the unfixed particles $n+1,\ldots,N$. The set of fixed coordinates can be used to describe a "reaction coordinate," $\xi(\mathbf{r}_1,\ldots,\mathbf{r}_n)$, and the PMF calculated as a function of ξ. Generally, the system will sample barriers in the free energy as a function of ξ infrequently, and methods to speed up the sampling of barriers have been developed: examples of techniques used in practice include umbrella sampling and the application of constraints to set appropriate values of the

Author complimentary copy. Redistribution subject to AIP license or copyright, see http://jcp.aip.org/jcp/copyright.jsp

reaction coordinate.[60] The method we use here is based on applying constraints through the "RATTLE" algorithm.[61] In considering the dissociation of an H-bonded dimer, we use the heavy atom to heavy atom distance[62] as the reaction coordinate.

Beginning with the suggestion in Ref. 24, PMFs have been used within the path integral formalism for studying reactions and proton transfers.[39,63–71] They have not however been widely deployed in simulations employing *ab initio* electronic structure calculations. The connection allowing the application of constraint algorithms within a PIMD simulation is provided by the centroids. In a standard application of RATTLE in an MD simulation with classical nuclei, at each step of the run, corrections to the positions and velocities are determined, which ensure that the specified constraints are satisfied. In the PIMD version, at each step, we calculate the centroid positions and velocities, use RATTLE to determine appropriate corrections, and uniformly adjust the coordinates of the constrained atoms in each of the beads according to these corrections. Previous applications combining centroid constraints and *ab initio* electronic structure methods include the study by Tuckerman and Marx[72] of proton transfer along H-bonds in malonaldehyde, the study of proton transfer in $BaZrO_3$ by Zhang *et al.*,[73] and the studies of proton transfer reactions by Xiang and Warshel[74] and Major *et al.*[75]

We have modified the PIMD routines of the CASTEP code to allow the application of constraints to the centroids; the additional computer code required on top of the existing PIMD/DFT implementation is minimal, and the computational workload needed to gather sufficient statistics to converge the mean forces is manageable. We have carefully tested our implementation of the constrained-centroid algorithm (for details, see the supplementary material[76]). In the constrained classical nucleus MD simulations, the existing implementation of RATTLE for constraining classical nuclei in CASTEP is used.[77] The Born–Oppenheimer scheme is used to perform the MD and PIMD simulations. We use 16 beads (with staging coordinates[78]) in the PIMD simulations of $(HF)_2$ and $(H_2O)_2$.[77]

III. HF DIMER

The first H-bonded system to which we apply our methodology is the HF dimer, where two HF monomers are held together by a single H-bond. This system has been studied in several earlier works, e.g., Refs. 45 and 46, and in particular with PBE DFT in Ref. 48. Unconstrained classical nucleus MD and PIMD simulations are performed at $T=50$ K. The dimer remains stable during both of these unconstrained simulations. Once the unconstrained calculations are equilibrated, constrained simulations are performed in which the F–F distance is held fixed, while the H atoms are free to move. For the longest F–F distance considered in the constrained runs, the individual HF monomers are clearly well separated. We present cumulative averages[79] of the constraint forces for the HF dimer calculated with the classical and PIMD treatments of the nuclei in Fig. 1. The final mean

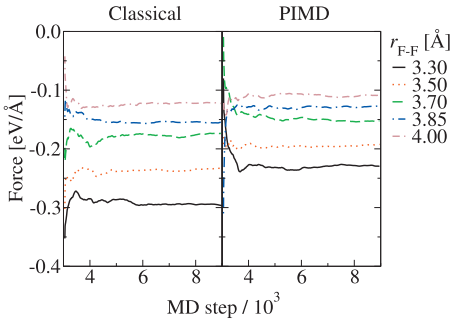

FIG. 1. Cumulative averages (taken from step 3000) of the constraint forces for the HF dimer with various values of the F–F spacing, as obtained from constrained classical nucleus MD (left panel) and constrained-centroid PIMD (right panel) simulations at $T=50$ K. The F–F spacings are 3.30 Å (black solid line), 3.50 Å (red dotted line), 3.70 Å (green long-dashed line), 3.85 Å (blue dot-long-dashed line), and 4.00 Å (brown dot-double-dashed line).

forces are shown in Fig. 2. As far as we are aware, mean force curves for the dissociation of H-bonds have not previously been calculated using PIMD with *ab initio* electronic structures.

The mean forces obtained from the simulations (Figs. 1 and 2) with the nuclei treated classically and quantum-mechanically show clear differences. To check the convergence of our PIMD calculations with respect to the number of PIMD beads, we include the mean forces calculated using 32 beads for F–F distances of 3.0 and 4.0 Å in Fig. 2. The 32 bead PIMD mean forces agree very well with those calculated using 16 beads.

Integrating each force profile in Fig. 2 from the point where it crosses zero provides the corresponding effective free energy profile.[80] In the limit of large spacings, this gives estimates of the free energies of dissociation, which are shown in Table II as ΔF^{class} for the constrained classical nucleus MD and ΔF^{PIMD} for the constrained-centroid PIMD simulations.

The free energy of dissociation is reduced upon inclusion of quantum nuclei by 26%, indicating that the bonding of the HF molecules in the dimer is weaker when the quan-

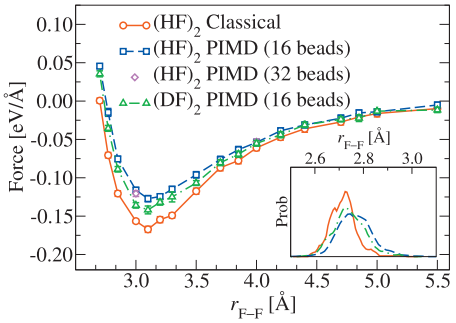

FIG. 2. Mean constraint forces for the HF dimer vs F–F spacing from constrained classical nucleus MD (red circles/solid line) and constrained-centroid PIMD (blue squares/dashed line) simulations at $T=50$ K. The magenta diamonds show constrained-centroid PIMD mean forces calculated with 32 beads. The constrained-centroid PIMD profile for the DF dimer is shown by the green triangles/dot-dashed line. The inset shows the distribution of unconstrained F–F distances for $(HF)_2$ with classical nuclei (solid red line), $(HF)_2$ with PIMD (dashed blue line), and $(DF)_2$ with PIMD (dot-dashed green line).

Author complimentary copy. Redistribution subject to AIP license or copyright, see http://jcp.aip.org/jcp/copyright.jsp

TABLE II. Energy changes upon dissociation of the $(HF)_2$ and $(DF)_2$ dimers. The energies are ΔF^{class}, free energy difference obtained from classical nucleus MD; ΔF^{PIMD}, free energy difference obtained from PIMD; D_e, difference in the DFT internal energies between bound dimer and separate monomers; and ΔZPE, difference in the harmonic zero-point energy.

Energy (eV)	$(HF)_2$	$(DF)_2$
ΔF^{class}	0.212	0.205
ΔF^{PIMD}	0.157	0.183
D_e	0.238	
ΔZPE	0.084	0.065
$D_e - \Delta\text{ZPE}(=D_0)$	0.153	0.173

tum mechanics of the nuclei is included. The distributions of F–F distances from unconstrained simulations are included in the inset of Fig. 2 and illustrate that the inclusion of quantum nuclear effects leads to an increased equilibrium F–F distance: the average F–F distance obtained from the classical nucleus MD simulation is $r_{\text{F–F}}=2.72$ Å and that from the PIMD simulation is $r_{\text{F–F}}=2.77$ Å, an increase in the PIMD case of 2%. The reduction in H-bond strength found by direct calculation of the free energy of dissociation is consistent with the increased F–F distance in the unconstrained PIMD simulations.

A consistency check between the constrained mean force calculations and the unconstrained results is provided by comparing the F–F distance at which the mean force curves cross zero, with the average heavy atom distances found in the unconstrained simulations. For the HF dimer, the mean force curve crosses zero at an F–F spacing of about 2.70 Å in the classical case and 2.75 Å in the PIMD case, both in good agreement with the values obtained from the unconstrained simulations.

To investigate further the observation that quantum nuclear effects weaken the H-bond, we consider the HF dimer model with the hydrogen atoms replaced by deuterium (D) atoms. We expect that with the heavier deuterium atoms, the influence of the quantum mechanics of the nuclei should be reduced with respect to regular H, and the difference between the free energies of dissociation calculated with PIMD and classical nucleus MD should correspondingly be reduced.

In Fig. 2, we show the PIMD mean forces calculated for the DF dimer. As for the HF dimer, the inclusion of quantum nuclear effects reduces the dissociation free energy for the DF dimer, but by a smaller amount (11%), consistent with the reduced quantum nuclear effects in the DF dimer. In unconstrained simulations of $(DF)_2$, the PIMD average F–F distance is $r_{\text{F–F}}=2.74$ Å, an increase over the classical nucleus MD value of 1%, a smaller increase than that observed in the HF dimer case. The PIMD mean force curve crosses zero at an F–F spacing of 2.74 Å, in agreement with the unconstrained PIMD simulation.

The ratio of the change in the free energy of dissociation due to quantum nuclei in $(HF)_2$ to that in $(DF)_2$ is 2.5, which matches the ratio of the changes in the F–F distances in $(HF)_2$ and $(DF)_2$. The correspondence between these ratios lends support to the inferences made in an earlier work that

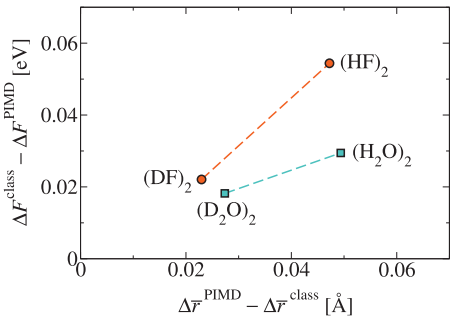

FIG. 3. Changes in the free energy of dissociation due to quantum nuclear effects vs change in the average heavy atom distances.

an increase in the bond length upon the inclusion of quantum nuclei corresponds to a weakening of the H-bond. In Fig. 3, we show the change in free energy of dissociation due to quantum nuclear effects versus the change in the average F–F distance (from the unconstrained simulations) for the HF and DF dimers. Although the data are limited, the points are consistent with the expectation that as the atomic masses become larger, $\Delta F^{\text{class}} - \Delta F^{\text{PIMD}}$ and $\Delta\bar{r}^{\text{PIMD}} - \Delta\bar{r}^{\text{class}}$ tend to zero together.

IV. WATER DIMER

We now consider the water dimer, again comparing classical nucleus MD and PIMD calculations at $T=50$ K. The dimer remains stable in unconstrained simulations made using both methods. The classical nucleus MD simulation gives the equilibrium O–O distance as $r_{\text{O–O}}=2.90$ Å, and the PIMD simulation gives $r_{\text{O–O}}=2.96$ Å, an increase in the PIMD case of 2%.

We then calculate the mean forces[79] at various O–O spacings with PIMD and classical nucleus MD, obtaining the curves in Fig. 4, and integrate[80] to obtain the free energy of dissociation. When quantum nuclei are introduced, there is a reduction in the free energy of dissociation, signaling a weaker H-bond. For the water dimer, the inclusion of quantum nuclei reduces the free energy of dissociation by 16% (Table III), a substantial reduction, although smaller than that seen for the HF dimer.

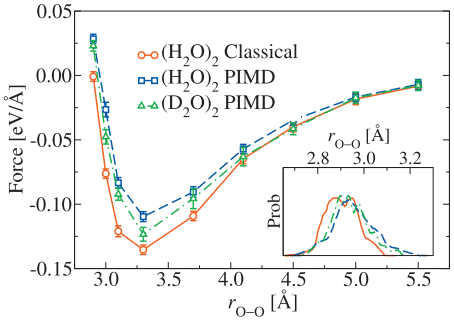

FIG. 4. Mean constraint forces for the water dimer vs O–O spacing from constrained classical nucleus MD (red circles/solid line) and constrained-centroid PIMD (blue squares/dashed line) simulations at $T=50$ K. The dot-dashed green line shows the mean forces for the D_2O dimer obtained with the PIMD treatment. The inset shows distributions of O–O distances obtained from unconstrained classical nucleus MD (red solid line) and PIMD (blue dashed line) simulations of H_2O and from a PIMD simulation (green dot-dashed line) of D_2O.

Author complimentary copy. Redistribution subject to AIP license or copyright, see http://jcp.aip.org/jcp/copyright.jsp

TABLE III. Energy changes upon dissociation of the $(H_2O)_2$ and $(D_2O)_2$ dimers. The energies are labeled as in Table II.

Energy (eV)	$(H_2O)_2$	$(D_2O)_2$
ΔF^{class}	0.184	0.180
ΔF^{PIMD}	0.155	0.162
D_e	0.232	
ΔZPE	0.110	0.075
$D_e - \Delta\text{ZPE}(=D_0)$	0.122	0.157

The mean force curves for the water dimer cross zero at O–O spacings of 2.90 and 2.95 Å in the classical nucleus and PIMD cases, respectively, matching well the corresponding unconstrained simulations. With the hydrogen atoms in the water dimer replaced by deuterium atoms to form $(D_2O)_2$, the reduction in the free energy of dissociation in the PIMD calculation with respect to the classical nucleus calculation is 10%. The changes in the free energy of dissociation due to quantum nuclei are plotted versus the change in the average O–O distance due to quantum nuclei for $(H_2O)_2$ and $(D_2O)_2$ in Fig. 3.

V. DISCUSSION AND CONCLUSIONS

We have directly calculated the free energy changes involved in dissociating the H-bonds of two dimers, $(HF)_2$ and $(H_2O)_2$, at 50 K, with classical and quantum treatments of the nuclei. For both dimers, including quantum nuclear effects through PIMD raises the mean force curve above that calculated using classical nucleus MD (Figs. 2 and 4) and decreases the absolute value of the free energy of dissociation with respect to the classical nucleus result (Tables II and III). For the HF dimer, quantum nuclear effects reduce the dissociation free energy by 26%, while in the water dimer, they reduce the dissociation free energy by 16%, in both cases significantly weakening the H-bond. The differences in the dissociation free energy suggest that the influence of quantum nuclear effects is somewhat larger in the HF dimer than the water dimer at the temperature considered. Further free energy calculations indicate that the reduction in bond strength due to quantum nuclear effects is smaller for both dimers when the hydrogen atoms are replaced by deuterium atoms: to 11% for $(DF)_2$ and 10% for $(D_2O)_2$. The weakening of the H-bonds seen in the dissociation free energies correlates well with the weakening of the H-bond structures suggested by longer average heavy atom distances in these dimers found in unconstrained PIMD and classical nucleus MD simulations. The inclusion of quantum nuclear effects increases the heavy atom average distances by ~2% for both dimers.

For the HF dimer, the harmonic zero-point corrected dissociation energy D_0 (Ref. 52) (see Table I) provides a good estimate of the PIMD free energy of dissociation ΔF^{PIMD} at $T=50$ K, obtained from the constrained-centroid PIMD simulations, with D_0 underestimating ΔF^{PIMD} by ~3%. For the water dimer, D_0 provides a ball-park estimate of the free energy of dissociation, although it underestimates F^{PIMD} by 21%. Discrepancies between D_0 and ΔF^{PIMD} are expected to be due to anharmonic effects, which are not captured in D_0. The deviations for both the HF and water dimers are relatively small, consistent with harmonic effects being dominant near the minimum energy structures of the dimer and separate monomers; we might expect larger disagreement between D_0 and F^{PIMD} in more anharmonic situations. The values also suggest that anharmonic effects are more important in the water dimer than in the HF dimer.

Our work shows that despite being quite computationally intensive, the dissociation free energies of H-bonds with quantum nuclear effects taken into account can now be handled at an *ab initio* level. Furthermore, we have directly observed the correlation between increased atomic distances and weakening of the H-bonds due to quantum nuclear effects, for the dimers considered, $(HF)_2$ and $(H_2O)_2$, at the temperature considered, 50 K.

ACKNOWLEDGMENTS

This work was supported by the European Research Council. A.M. is also supported by the EURYI award scheme (see www.esf.org/euryi) and the EPSRC-GB. We are grateful to the London Centre for Nanotechnology and UCL Research Computing for providing computational resources. Via our membership of the U.K.'s HPC Materials Chemistry Consortium, which is funded by EPSRC-GB (Grant No. EP/F067496), we made use of the facilities of the U.K.'s national high-performance computing services HPCx (provided by EPCC at the University of Edinburgh and by STFC Daresbury Laboratory, and funded by the Department for Innovation, Universities and Skills through EPSRC's High End Computing Programme) and HECToR (provided by UoE HPCx, Ltd., at the University of Edinburgh, Cray, Inc., and NAG, Ltd., and funded by the Office of Science and Technology through EPSRC's High End Computing Programme). The authors would like to thank Dr. Matt Probert for helpful discussions.

[1] Y. Maréchal, *The Hydrogen Bond and the Water Molecule* (Elsevier, New York, 2007).
[2] R. A. Kuharski and P. J. Rossky, J. Chem. Phys. **82**, 5164 (1985).
[3] B. Chen, I. Ivanov, M. L. Klein, and M. Parrinello, Phys. Rev. Lett. **91**, 215503 (2003).
[4] J. C. Grossman, E. Schwegler, E. W. Draeger, F. Gygi, and G. Galli, J. Chem. Phys. **120**, 300 (2004).
[5] E. Schwegler, J. C. Grossman, F. Gygi, and G. Galli, J. Chem. Phys. **121**, 5400 (2004).
[6] P. Wernet, D. Nordlund, U. Bergmann, M. Cavalleri, M. Odelius, H. Ogasawara, L. Å. Näslund, T. K. Hirsch, L. Ojamäe, P. Glatzel, L. G. M. Pettersson, and A. Nilsson, Science **304**, 995 (2004).
[7] D. Prendergast, J. C. Grossman, and G. Galli, J. Chem. Phys. **123**, 014501 (2005).
[8] L. Hernández de la Peña and P. G. Kusalik, J. Am. Chem. Soc. **127**, 5246 (2005).
[9] G. S. Fanourgakis, G. K. Schenter, and S. S. Xantheas, J. Chem. Phys. **125**, 141102 (2006).
[10] H.-S. Lee and M. E. Tuckerman, J. Chem. Phys. **125**, 154507 (2006).
[11] M. V. Fernández-Serra and E. Artacho, Phys. Rev. Lett. **96**, 016404 (2006).
[12] F. Paesani, S. Iuchi, and G. A. Voth, J. Chem. Phys. **127**, 074506 (2007).
[13] J. A. Morrone and R. Car, Phys. Rev. Lett. **101**, 017801 (2008).
[14] D. Marx and J. Hutter, in *Modern Methods and Algorithms of Quantum Chemistry*, NIC Series Vol. 3, edited by J. Grotendorst (John von Neumann Institute for Computing, Jülich, 2000), pp. 329–477.
[15] X.-Z. Li, M. I. J. Probert, A. Alavi, and A. Michaelides, Phys. Rev. Lett.

Author complimentary copy. Redistribution subject to AIP license or copyright, see http://jcp.aip.org/jcp/copyright.jsp

104, 066102 (2010).
[16] K. Kuchitsu and K. Oyanagi, Faraday Discuss. Chem. Soc. **62**, 20 (1977).
[17] S. Raugei and M. L. Klein, J. Am. Chem. Soc. **125**, 8992 (2003).
[18] D. C. Clary, D. M. Benoit, and T. van Mourik, Acc. Chem. Res. **33**, 441 (2000).
[19] C. Swalina, Q. Wang, A. Chakraborty, and S. Hammes-Schiffer, J. Phys. Chem. A **111**, 2206 (2007).
[20] J. G. Kirkwood, J. Chem. Phys. **3**, 300 (1935).
[21] E. Guàrdia, R. Rey, and J. A. Padró, Chem. Phys. **155**, 187 (1991).
[22] B. Roux, Comput. Phys. Commun. **91**, 275 (1995).
[23] M. Sprik and G. Ciccotti, J. Chem. Phys. **109**, 7737 (1998).
[24] M. J. Gillan, J. Phys. C **20**, 3621 (1987).
[25] M. E. Tuckerman, in *Quantum Simulations of Complex Many-Body Systems: From Theory to Algorithms*, NIC Series Vol. 10, edited by J. Grotendorst, D. Marx, and A. Muramatsu (John von Neumann Institute for Computing, Jülich, 2002), pp. 269–298.
[26] S. Miura, M. E. Tuckerman, and M. L. Klein, J. Chem. Phys. **109**, 5290 (1998).
[27] D. Marx, M. E. Tuckerman, and G. J. Martyna, Comput. Phys. Commun. **118**, 166 (1999).
[28] E. Geva, Q. Shi, and G. A. Voth, J. Chem. Phys. **115**, 9209 (2001).
[29] P. Durlak, C. A. Morrison, D. S. Middlemiss, and Z. Latajka, J. Chem. Phys. **127**, 064304 (2007).
[30] J. Cao and G. A. Voth, J. Chem. Phys. **101**, 6168 (1994).
[31] J. Cao and G. A. Voth, J. Chem. Phys. **100**, 5106 (1994).
[32] J. Cao and G. J. Martyna, J. Chem. Phys. **104**, 2028 (1996).
[33] M. Pavese, D. R. Berard, and G. A. Voth, Chem. Phys. Lett. **300**, 93 (1999).
[34] M. Pavese, S. Jang, and G. A. Voth, Parallel Comput. **26**, 1025 (2000).
[35] A. Witt, S. D. Ivanov, M. Shiga, H. Forbert, and D. Marx, J. Chem. Phys. **130**, 194510 (2009).
[36] I. R. Craig and D. E. Manolopoulos, J. Chem. Phys. **121**, 3368 (2004).
[37] I. R. Craig and D. E. Manolopoulos, J. Chem. Phys. **122**, 084106 (2005).
[38] A. Pérez, M. E. Tuckerman, and M. H. Müser, J. Chem. Phys. **130**, 184105 (2009).
[39] R. Collepardo-Guevara, Y. V. Suleimanov, and D. E. Manolopoulos, J. Chem. Phys. **130**, 174713 (2009).
[40] D. Vanderbilt, Phys. Rev. B **41**, 7892 (1990).
[41] DFT calculations for the HF and water dimers are made using plane wave basis sets specified by the cutoff energy E_{cut}=400 eV. An energy convergence criterion of 10^{-7} eV/atom was used for the DFT calculation made at each time step in the MD and PIMD simulations.
[42] M. C. Payne, M. P. Teter, D. C. Allan, T. A. Arias, and J. D. Joannopoulos, Rev. Mod. Phys. **64**, 1045 (1992).
[43] J. P. Perdew, K. Burke, and M. Ernzerhof, Phys. Rev. Lett. **77**, 3865 (1996).
[44] S. J. Clark, M. D. Segall, C. J. Pickard, P. J. Hasnip, M. J. Probert, K. Refson, and M. C. Payne, Z. Kristallogr. **220**, 567 (2005).
[45] C. Tuma, A. D. Boese, and N. C. Handy, Phys. Chem. Chem. Phys. **1**, 3939 (1999).
[46] K. N. Rankin and R. J. Boyd, J. Comput. Chem. **22**, 1590 (2001).
[47] J. Ireta, J. Neugebauer, M. Scheffler, A. Rojo, and M. Galván, J. Phys. Chem. B **107**, 1432 (2003).
[48] J. Ireta, J. Neugebauer, and M. Scheffler, J. Phys. Chem. A **108**, 5692 (2004).
[49] B. Santra, A. Michaelides, and M. Scheffler, J. Chem. Phys. **127**, 184104 (2007).
[50] B. Santra, A. Michaelides, M. Fuchs, A. Tkatchenko, C. Filippi, and M. Scheffler, J. Chem. Phys. **129**, 194111 (2008).
[51] B. Santra, A. Michaelides, and M. Scheffler, J. Chem. Phys. **131**, 124509 (2009).
[52] The equilibrium dissociation energy of a dimer D_e is calculated by subtracting the total energy of the fully relaxed dimer from that of two separate fully relaxed monomers, i.e., twice the total energy of a single fully relaxed monomer. The harmonic ZPE is calculated using the harmonic frequencies $\{\omega_i\}$ corresponding to the relaxed structure via ZPE $=\frac{1}{2}\hbar\Sigma_i\omega_i$, and the change in ZPE for dimer dissociation, ΔZPE, is calculated by subtracting the ZPE of the fully relaxed dimer from that of two separate fully relaxed monomers. The ZPE-corrected dissociation energy is then obtained as $D_0=D_e-\Delta$ZPE.
[53] For our static dissociation energy calculations, we use cubic supercells with side length of 12.0 Å. All Brillouin zone integrations are performed using the gamma point.
[54] P. Jurečka, J. Šponer, J. Černý, and P. Hobza, Phys. Chem. Chem. Phys. **8**, 1985 (2006).
[55] G. S. Tschumper, M. D. Kelty, and H. F. Schaefer III, Mol. Phys. **96**, 493 (1999).
[56] W. Klopper, J. G. C. M. van Duijneveldt-van de Rijdt, and F. B. van Duijneveldt, Phys. Chem. Chem. Phys. **2**, 2227 (2000).
[57] T. Bucko, J. Phys.: Condens. Matter **20**, 064211 (2008).
[58] A. Jezierska and J. J. Panek, J. Chem. Theory Comput. **4**, 375 (2008).
[59] A. Jezierska and J. J. Panek, J. Comput. Chem. **30**, 1241 (2009).
[60] D. Trzesniak, A.-P. E. Kunz, and W. F. van Gunsteren, ChemPhysChem **8**, 162 (2007).
[61] H.-C. Andersen, J. Comput. Phys. **52**, 24 (1983).
[62] The simulations show that the average distance between the H atom participating in the H-bond and the H-bond acceptor atom scales linearly with the heavy atom to heavy atom distance. Thus, we could equally well plot the mean forces in Figs. 2 and 4 as functions of the H to acceptor distance and perform the free energy analysis in terms of this length instead of the heavy atom distance, though the results would be the same.
[63] G. A. Voth, D. Chandler, and W. H. Miller, J. Chem. Phys. **91**, 7749 (1989).
[64] J. S. Bader, R. A. Kuharski, and D. Chandler, J. Chem. Phys. **93**, 230 (1990).
[65] Y. C. Sun and G. A. Voth, J. Chem. Phys. **98**, 7451 (1993).
[66] H. Azzouz and D. Borgis, J. Chem. Phys. **98**, 7361 (1993).
[67] J. Lobaugh and G. A. Voth, J. Chem. Phys. **100**, 3039 (1994).
[68] T. R. Mattsson, U. Engberg, and G. Wahnström, Phys. Rev. Lett. **71**, 2615 (1993).
[69] S. Consta and R. Kapral, J. Chem. Phys. **101**, 10908 (1994).
[70] J. Lobaugh and G. A. Voth, J. Chem. Phys. **104**, 2056 (1996).
[71] D. T. Major and J. Gao, J. Am. Chem. Soc. **128**, 16345 (2006).
[72] M. E. Tuckerman and D. Marx, Phys. Rev. Lett. **86**, 4946 (2001).
[73] Q. Zhang, G. Wahnström, M. E. Björketun, S. Gao, and E. Wang, Phys. Rev. Lett. **101**, 215902 (2008).
[74] Y. Xiang and A. Warshel, J. Phys. Chem. B **112**, 1007 (2008).
[75] D. T. Major, A. Heroux, A. M. Orville, M. P. Valley, P. F. Fitzpatrick, and J. Gao, Proc. Natl. Acad. Sci. U.S.A. **106**, 20734 (2009).
[76] See supplementary material at http://dx.doi.org/10.1063/1.3505038 for details of tests of the constrained-centroid method in the classical regime. Mean forces calculated using constrained classical nuclei and constrained-centroid PIMD are compared for the example molecule, Si_2H_2, at 1000 K.
[77] For the HF and water dimers, all PIMD and MD simulations are made using an integration time step of 0.7 fs, at a temperature of 50 K. In the PIMD calculations, each bead is thermostatted by a Langevin thermostat (Ref. 81). Langevin thermostats are also used to control temperature in the classical nucleus simulations. The PIMD calculations are performed using 16 beads. Cubic supercells having side length of 12.0 Å are used for dimer spacings up to 5.0 Å; for spacings greater than 5.0 Å, cubic supercells with side length of 18.0 Å are used. The largest drift in the average overall system energy [ion kinetic + DFT total energy (+ spring energy in the PIMD case)] observed in the MD and PIMD simulations was 0.006 eV/(ps atom), although generally the drifts observed in the simulations were well below 10^{-3} eV/ps atom.
[78] M. E. Tuckerman, B. J. Berne, G. J. Martyna, and M. L. Klein, J. Chem. Phys. **99**, 2796 (1993).
[79] In obtaining each final mean force value, we use at least 6000 MD steps (4.2 ps) after having discarded the first 3000 steps (2.1 ps).
[80] We have calculated mean forces at spacings of 5.5 and 9.0 Å using an 18.0 Å supercell (though these are not shown in Figs. 2 and 4) and checked that the mean forces calculated for dimer spacing of 5.5 Å with supercells of side length of 12.0 Å and 18.0 Å match. To obtain the energy changes upon dissociation, we have used the mean force values obtained using the 12.0 Å supercell for spacings up to and including 5.0 Å and the mean forces obtained using the 18.0 Å supercell for spacings of 5.5 and 9.0 Å.
[81] G. S. Grest and K. Kremer, Phys. Rev. A **33**, 3628 (1986).

Author complimentary copy. Redistribution subject to AIP license or copyright, see http://jcp.aip.org/jcp/copyright.jsp